

## **Liquid Surface Divertor Design for ARIES/CLIFF**

R.E. Nygren and M.A. Ulrickson, Sandia National Laboratories

B.E. Nelson and P.J. Fogarty, Oak Ridge National Laboratory

T.D. Rognlien and M.E. Rensink, Lawrence Livermore National  
Laboratory

J.N. Brooks, Argonne National Laboratory

S.S. Smolentsev, University of California, Los Angeles

### **Abstract**

The US Enabling Technology Program in fusion is investigating the use of free flowing liquid surfaces facing the plasma. We studied issues of integrating a liquid surface divertor into a configuration based upon an advanced tokamak, specifically the ARIES-RS configuration. One aspect of this work is developing workable liquid surface divertors that are incorporated into an overall design for a fusion chamber with flowing liquid walls. The simplest form of such a divertor is to extend the flow of the liquid first wall and avoid introducing any separate fluid streams. In this case, one can modify the flow above the divertor to enhance thermal mixing. One major consideration affecting the design is how MHD (magneto-hydrodynamics) affects the flowing liquid. In liquid metals, MHD can produce forces that redirect flow and suppress turbulence. An evaluation of Flibe (a molten salt) as a working fluid was done to assess a case in which the MHD forces could be largely neglected. Initial studies indicate that, for a tokamak with high power density, an integrated Flibe first wall and divertor does not seem workable. Sn and Sn-Li have also been considered and the initial evaluations on heat removal and plasma contamination show promise, although the complicated 3-D MHD flows cannot yet be fully modeled. Particle pumping in these design concepts is accomplished by conventional means (ports and pumps). However, trapping hydrogen in these flowing liquids seems plausible and novel concepts for entrapping helium are also being studied.

### **Introduction**

The practical issues of implementing a chamber design with liquid surfaces are being explored in the APEX (Advanced Power Extraction) Program[1]. There is also work on liquid surface plasma facing components being performed in the Advanced Limiter-divertor Plasma Facing Systems (ALPS) Program.[2]

The initial effort on divertor design in APEX has been to adapt the existing ARIES-RS design.[3] ARIES is a 2000MW D/T conceptual power plant design with a major radius of 5.5m, an aspect ratio of 4, a plasma current of 11MA and a density of  $2 \times 10^{20} \text{m}^{-3}$ . The alpha power to be exhausted in the scrape-off layer or (and) radiated is 400MW. The adaption for our liquid surface chamber includes two streams of flowing liquid. Nearer the plasma is a 2-cm thick first wall stream that is the immediate physical boundary outside the plasma. The upper portion of this stream is the first wall and at the bottom of the machine it becomes the divertor flow. Behind the first wall is a slower flowing liquid blanket

of Flibe or Li-Pb. This paper summarizes the various aspects of the current design and focuses on the work done for the divertor.

The work on the overall design is being reported elsewhere.[4] The mechanical design includes detailed CAD renderings and several innovative features. One example is a system of nozzles that launch the first wall flow. The nozzles are "self shielding" in that the flows overlap in a way that prevents line of sight from the plasma to the solid surface of a nozzle. Another innovation is the flexible "bag" of SiC that is used to guide the blanket flow stream and separate this from the flowing first wall. The temperatures of the flow streams are consistent with requirements for efficient power generation. The design effort includes an evaluation of safety concerns and state-of-the-art modeling, including modeling of the plasma edge, done within the overall APEX Program. Some information on the design is available in recent presentations for the APEX Program.[1] Fig. 1 shows the fluid flow path and some features of the design. In 1999 and early 2000, we studied Li and Flibe and in 2000 and 2001 we have been evaluating designs with Sn. Table 1 indicates some of the conclusions we reached in our preliminary assessments.

Table 1. Summary of ARIES/CLIFF Conclusions  
on Fluid Operating Temperature Windows for First wall and Divertor

	<u>Flibe</u>	<u>Li</u>	<u>Sn</u>
Max. allowable $T^*_{\text{surface}}$	~400°C	< 400°C	>700°C
Min. allowable fluid temperature	455°C	~200°C	~200°C
Inlet nozzles & penetrations	OK	MHD issues	MHD issues
First wall temp. window	none	small	large
Divertor temp. window	none	MHD issues	MHD issues
Vacuum pumping	OK	limited for He	TBD

\*wall limit, divertor limit under evaluation

We also recognize that Ga has higher thermal conductivity than Sn and is likely to have better power handling characteristics in the divertor. We will be evaluating the possible advantages in power handling in the divertor of Ga versus Sn in the future.

Interest in liquid surface divertors certainly did not begin with the APEX. The need to use Li to breed tritium for D-T fusion reactors led to the possibility that liquid Li might be used. The excellent heat transfer of liquid metals is well known and applied in heat pipes and in liquid metal fast breeder reactors, and liquid divertor designs with flowing films, jets, droplets and solid walls wetted have been proposed.[5-23] A gallium divertor was tested in the T-10 tokamak.[24]

A fundamental issue in treating liquid divertors is the power handling capability. Liquid metals have the added complications arising from liquid metal magneto-hydrodynamic (MHD) effects. To our knowledge the MHD issues have not been definitively addressed in any proposed fusion reactor designs to date where high power density is desired.

## Particle Handling in a Liquid Divertor

In our liquid surface designs, we presume vaporization from the liquid surfaces to be the primary source of plasma impurities. Since the vaporization rate is exponentially dependent upon temperature, there is a narrow range in which the impurity generation rate changes from moderate to unacceptable.

Plasma edge modeling by Rognlien and Rensink[25] with the 2D UEDGE code provides particle loads and the power deposition profiles in the ARIES/CLIFF divertor. Their modeling is complemented by that of Brooks using the BPHI-3D code, a sheath model with 3-D capability[26], to evaluate effects within the plasma sheath at the divertor.

The modeling has dealt with several aspects of the plasma edge that differ from more conventional machine operations, where measurements are also available to compare with the modeling. Ref. 25 describes early efforts in modeling Li walls in which the Li is assumed to be an active sink for hydrogen and severely reduces the recycling at the edge. For Li, the maximum fluid temperature limit based on a threshold level for the Li core impurity level in the model was about 380C for a low  $R_H$  of 0.25. The criterion for the maximum acceptable impurity level was that  $T_e$  at the wall collapsed and the solution was not stable for higher impurity influxes. Here the range of coolant temperature was judged to be too low for high efficiency in power generation; this conclusion was also tied to other analysis regarding a flowing Li blanket.

Subsequent work by Rognlien and Rensink[25] studies the penetration into the plasma of F, the most dangerous core-contamination component of Flibe. This modeling shows that, with high (0.98) hydrogen recycling ( $R_H$ ) and without some scheme other than simple pumping to enhance impurity removal at the edge, impurity contamination from Flibe would be problematic down to its melting point. (This modeling was done for an ITER divertor, that has more documentation than ARIES.) While some ideas for dealing with the edge impurities were advanced (e.g. heating the edge to mitigate radiation), effort on design was redirected to other fluids.

The development of ARIES/CLIFF has included designs with Li, Flibe and, most recently Sn or Ga, as candidates evaluated for the first wall and divertor stream. The Sn first wall and divertor appear in our initial evaluations to have a workable range in the fluid temperatures to make an attractive design. The type of modeling for the first wall mentioned above has also been done for Sn[26]. This yielded a maximum allowable temperature for a Sn first wall of 735°C for an  $R_H$  of 0.99. Figure 2 shows some sample results from UEDGE for a single null divertor with an assumed recycling of  $R_H$  of 0.98 and a high radiated fraction,  $f_{rad}$ , of 0.87. This high fraction of radiated power was included as an optimistic assumption that would help reduce the power load to the divertor, although a specific technique for achieving this was not included in the design. For a similar case, but with an  $f_{rad}$  of 0.74, the peak power rose to about 55MW/m<sup>2</sup>. Power

deposition profiles from the modeling were used for evaluation of the thermal performance of the divertor as described later.

With regard to the maximum allowable surface temperature in a Sn divertor, a higher allowable temperature is possible since a more difficult path is anticipated for impurities from the divertor to come back into the core plasma than for impurities from the first wall. In the specific case of thermal impurities launched by vaporization, only a tiny fraction of the atoms ever escape the sheath, i.e., the mean free path for ionization of the slow evaporated Sn atoms is small compared to the thickness of the sheath. Table 1 shows results of sheath modeling by Brooks for evaporated Sn for typical "high recycling" divertor conditions. Here a less rigorous treatment than the full 3-D power of the code is used; for example, lateral gradients in surface temperature and plasma properties are ignored and the surface is presumed to be of uniform temperature. The criterion is that the solution must be stable for a time equal to the time it takes the flowing liquid to pass through the strike zone of the divertor. This is typically a few milliseconds for a fluid flowing at 10m/s.

Table 1. Summary of Results by Brooks on Sheath Effect in Sn Divertor  
(calculation for an ITER-type divertor geometry)

$T_e = 30\text{eV}$ ,  $n_e = 3 \times 10^{20}/\text{m}^3$  at plasma/sheath boundary  
 $V_{th} = \sim 500\text{m/s}$  average emitted Sn atom velocity (thermal, @  $\sim 1700\text{K}$ )  
Debye length =  $2.35 \times 10^{-6}\text{m}$   
Sheath width ( $\sim 3 r_{gi}$ ) =  $5.3 \times 10^{-4}\text{m}$   
Mean-free-path for emitted atom ionization ( $\perp$ ) =  $3.61 \times 10^{-5}\text{m}$   
D-T ion particle flux,  $\Gamma_{DT} = 3.77 \times 10^{23}/\text{m}^2\text{-s}$   
 $\Gamma_{Sn} = 0.2\Gamma_{DT}$ , steady-state criterion for whole-surface evaporation  
Maximum evaporated Sn flux =  $7.54 \times 10^{22}/\text{m}^2\text{-s}$   
Surface temperature limit for above flux =  $\sim 1300^\circ\text{C}$

Using the results above and extrapolation from sheath/thermal studies[27,28], one of us (Brooks) estimates that a large local vaporization rate of Sn equal to  $\sim 20\%$  of the incoming DT particle flux still results in an acceptable level of Sn escaping from the sheath, i.e., the impurity source term at the plasma boundary above the sheath. This limit corresponds to the evaporation rate (and thermal velocity) of Sn at  $\sim 1300^\circ\text{C}$ . We estimate also a rough "allowable value" of  $\sim 1600^\circ\text{C}$  for the maximum temperature of a "hot spot" with a 1cm diameter.

For pumping of He, the divertor at present uses a conventional approach with exhaust ports and pumps. This has been incorporated by providing lateral ports in the lower portion of the first wall and larger exhaust ducts at the bottom that serve to collect the fluid stream and provide pumping. Toroidal breaks near the bottom of the first wall (see Fig. 1) move the fluid flow around the opening of the exhaust ducts. The ducts were sized to provide adequate total conductance (lateral and downward ducts) for the modeled D/T throughput and pressure in the divertor of  $\sim 3\text{mTorr}$ . The He pumping was judged adequate based on 2-D

modeling of the He density in a high recycling divertor (which we assume for liquid Sn) and adequate pumping of the D/T.

Some novel ideas for trapping helium in the fluid surface are also being investigated. The notions tend to defy the conventional wisdom that one expunges He from solid metals by melting them, and calculations indicate that the trapped fluence would be small. However some hope may exist that He release might be slowed by defects (impurities) or bubble formation.

### **Power Handling - issues**

The goal of high power density presents challenging engineering, and this is especially true for the power handling in a divertor because the total power scales with the plasma volume ( $\sim \text{radius}^3$ ) while the area on which power is deposited in the divertor scales approximately with the radius<sup>2</sup>. Of course other factors such as the plasma scrape-off length, flux expansion and target angle also affect the power density in the divertor, but the optimized combination of these factors for a solid-surface divertor is likely to be similar for a given confinement scheme (e.g. tokamaks).

For a flow of 10m/s, the transit time for flow down the  $\sim 8\text{m}$  poloidal length of the first wall is 0.8s. Although there is a rise in temperature from top to bottom, two of us (Rognlien and Rensink) have shown the rate of impurity generation for the first wall can be fairly well estimated by using the average first wall temperature in calculating the impurity source. For the first wall, the dominant effect in impurity generation is its very large area.

The simplest scheme for the divertor is to use a continuation of the first wall flow and thereby eliminate the set of nozzles and plumbing needed to introduce another coolant stream. A consequence of this simplicity is that, upstream to the divertor, the coolant stream has already collected heat as the first wall and established a commensurate thermal gradient at the surface of the fluid. The duration that a fluid element at the surface of the divertor flows across the peaked heat load is only a few milliseconds. The short exposure is the reason that relatively high peak heats loads can be considered with liquid surface divertors.

Flibe, with its low electrical conductivity, was evaluated with the initial hope that the disadvantage of its low thermal conductivity might be mitigated in part by turbulent flow, and its beneficial effect on heat transfer. (Whereas we expect the suppression of classical turbulence in liquid metals due to MHD effects.) Smolentsev modeled the effect of turbulence on heat transfer in Flibe[29,30], and a sample result is shown later. As noted above, the overall results for Flibe were not encouraging for the specific high power density design in ARIES/CLIFF.

For liquid metals (e.g., Li, Sn, Sn-Li or Ga), their inherent high thermal conductivity means that there would be relatively less contribution from turbulence to assist in the penetration of heat from the heated surface into the fluid. MHD forces tend to force the fluid to flow en masse ("slug flow") like a

sliding plate and the basic problem (oversimplified) is essentially similar to heating a plate from one side. The first wall flow "integrates" the heat load along the poloidal flow path and builds a commensurate temperature gradient at the surface.

The first wall flow "integrates" the heat load along the poloidal flow path and builds a commensurate temperature gradient at the surface. Were it possible to do so, some method thermal mixing would be desirable before the fluid stream from the first wall becomes the divertor flow. This thermal mixing differs from natural turbulence in that the cell size for the modification is large. We want to redirect the surface layer of several millimeters and thermally mix it with the cooler fluid below, or redirect it so that cooler fluid is exposed in the modified stream.

We believe it will be possible to accomplish this and the divertor layout shown later is a first attempt. However, 3-D MHD effects will be important in the flow and, as yet, we are not modeling these effects. In the ARIES-RS divertor, the field has roughly equal components in the toroidal and poloidal directions. Also, as the fluid passes into the steep gradient in heat flux that corresponds to penetration of the scrape-off-layer and the surface temperature rises rapidly, the fluid is crossing flux lines, and the field gradients in the radial direction are important. So, the MHD effects arise from a somewhat complicated geometry.

### **Power Handling - Coolant Capabilities and Basic Data**

A general assessment of heat flux limits for flowing liquid surfaces composed of either Li or Sn75Li25 (Sn-Li) was done (Ulrickson) for the first wall. Calculations for surfaces of pure Sn, In and Ga were included for divertor surface applications. The models use laminar flow and the best estimates of the surface temperature limits from plasma modeling. Any turbulence would tend to reduce the surface temperatures. However, the experimental evidence from the Russian tokamaks supports laminar flow. We are not aware of experiments in which induced currents are used to mix the flow. Where the thermal properties are not known, e.g., Sn-Li, we have tried to use conservative values in the estimated properties. Some further remarks on the properties of Sn are given later.

Heat load limits were developed based upon surface temperature limits associated with the acceptable level of plasma impurity. The Rognlien/Rensink surface temperature limits were used for Li and Sn-Li. For Sn, In and Ga, allowed concentrations and associated surface temperatures were based on an allowable limit scaling with  $Z^3$  or a possible limiting value from the collapse of the sheath due to ionization of the evaporated material. The limiting values for  $Z^3$  scaling were 600°C for Sn and Ga and 500°C for In. The Brooks estimate of the limit for Sn for sheath collapse is ~1000°C (first wall). The equivalent evaporation rates for In and Ga occur at 800°C and 850°C respectively. The first estimate (lower temperatures) gives a likely lower bound for an allowable

duration of exposure or limiting heat flux. The second estimate gives a likely an upper bound.

Figures 3-5 show the results. The time required to reach the temperature limit was determined for a given constant heat flux and temperature-dependent material properties. The starting temperature was 40°C above the melting point.

Li and Sn-Li have similar behavior. The lower end of the estimated values for Sn-Li is about a factor of two below the higher values (Fig. 3). Sn-Li has a wider temperature window than Li but the thermal properties are poorer and the performance limits are nearly identical. The allowed duration is inversely proportional to the square of the heat flux. For the lower bound temperature limit (Fig. 4) both pure Sn and pure In are very similar to Li. Gallium shows a substantial advantage over the other materials. For the upper bound (Fig. 5), Sn and In have an advantage over Li, but Ga is clearly superior again.

Analyses of the effect of the divertor angle and flow velocity were also performed and cases with the peaked heat flux profile for ITER were analyzed. The conclusions are as follows. Li and Sn-Li appear from these estimates to have very similar heat flux windows of operation, but Sn-Li could have poorer performance if the thermal properties are at the lower limits estimated. The thermal properties of molten Sn-Li alloys need to be measured to reduce the uncertainty of these calculations. Gallium appears to have a considerable advantage over all the other materials from a thermal performance standpoint. Other factors such as cost, activation and corrosion will need to be considered.

Even the basic thermophysical data for these design studies is an “R&D issue” at this point. One might expect that the properties of a liquid alloy such as Sn-Li are not well studied, but we also had difficulty finding data on liquid metal elements in the temperature ranges of interest for our fusion applications. Experimental data on the thermophysical properties of liquid Sn are available over only a limited range and there can be pitfalls in extrapolating any such data. For example, for the heat capacity,  $C_p$ , of liquid Sn, we found data over only a limited range of temperature, e.g. data compilations in Refs. 31-33. The following is an example of Nygren’s treatment of data to create a temperature dependent expression for the  $C_p$  of Sn for use in design evaluations of a Sn divertor.

A starting point was a parameter fit by Kubaschewski and Alcock.[34] Fig. 6 shows that data replotted as  $C_p(T)/C_p(T_m)$  versus homologous temperature ( $T/T_m$ ) for various liquid metals, where  $T_m$  is the melting temperature. In this figure the limited extent of the Sn data are shown, as are the trend curves for various other liquid metals with more data. For Sn, one might expect the actual trend to rise again as is suggested by curves for Pb, or to stay rather flat, like the curve for Ga; but an extrapolation of the initial rapid decline seems inappropriate. In these data  $C_p$  drops quickly with temperature above the melting temperature over the short range of the data. *While theory in solid state physics may help in estimating the dependence of thermal conductivity on temperature there is less hope for such guidance for the heat capacity* -paraphrase from [33].

Data are also lacking at higher temperatures on the thermal conductivity,  $k$ , of liquid Sn, which rises significantly over the limited temperature range of available data. Based on arguments about what should happen near the critical temperature ( $\sim 8000\text{K}$ ) per Ho, Powell and Liley[35],  $k$  will stop increasing and decline at very high temperatures. The departure from linearity even at moderately high temperatures is important in our design because it means that the temperature limit for unacceptable evaporation is approached more rapidly with increasing heat flux than for a linear dependence on temperature. Figure 7 shows data from [35] and their recommended curve of  $k$  for liquid Sn (from the melting point to  $973\text{K}$  using a Lorentz<sup>1</sup> number of 0.02443 and values of the electrical resistivity at the end points of this range) plus a straight-line extrapolation. The  $k$ -REN (Nygren) curve in Fig. 7 uses the Ho, Powell and Liley formulation but substitutes values for electrical resistivity from Cusack and Enderby[36] for a range up to  $1473\text{K}$  and beyond that a further extrapolation of their data on resistivity to higher temperatures.

At this point, tin seems like a good candidate coolant based on its thermal properties. (The thermal properties of gallium suggest its heat handling capability would exceed that of tin, but we have not yet done evaluations beyond the analyses shown earlier.) As we hope is clear from the examples above, among the R&D needed for developing liquid surface divertors is additional basic data on thermophysical properties.

### **Power Handling – Heat Transfer**

The temperature profile along the surface of our liquid divertor is determined using power deposition profiles obtained from the UEDGE code for an ARIES-RS configuration with a single null divertor and the flow geometry of the ARIES/CLIFF design. The power deposition data in the divertor are fitted with a curve to represent the peaked profile with its steeper decline on the private flux side. One interesting feature of the modeling results in this regard was a broader tail on the power deposition profile than could be represented by a simple single exponential, as is normally used to describe the scrape-off layer.

We modify the power deposition from the 2-D model to account for some geometric factors, such as the toroidal openings in the outboard for the pump ducts. In this case, the power is simply redistributed on the remaining toroidal surface at this point. Also, for example, we have studied variations in the angle of inclination of the divertor, as described in the next section. But at this point we

---

<sup>1</sup> The Weidmann-Franz-Lorenz law, given below, relates thermal conductivity to electrical conductivity (for metals). The Lorenz number (0.0245) is a theoretically derived constant but experimental values are found to deviate somewhat.

$$\frac{k}{\sigma_e T} = 0.0245 \quad (W\mu\Omega/K^2)$$

simply keep the power deposition along the field lines the same rather than requesting individual UEDGE modeling runs for each case.

Fig. 8 shows the result from an early calculation (Smolentsev) of the surface temperature along the flow path of a liquid Flibe first wall and outboard divertor with an initial flow velocity of 10m/s. The first wall receives  $2\text{MW}/\text{m}^2$  and the peak power on the outboard divertor, which receives 60% of the heat, is about  $55\text{MW}/\text{m}^2$ . In this particular case, the heat load has been multiplied by 1.6 for a probably over-generous allowance of 40% of the toroidal surface in the divertor for pumping ports. (The effect of partial suppression of turbulence due to MHD effects on Flibe as represented in the  $k-\varepsilon$  turbulent heat transfer model was studied.[29,30] )

In this early case, there is no flow modification per sec in the transition to the divertor but an allowance was made by using a (non-physical) zero heat load in this region. Thus, the plot indicates a relaxation of the surface temperature relaxation in this region. We have not yet completed calculations for the newer divertor configuration described in the next section.

### **Divertor Configuration**

In developing a divertor configuration, the starting envelope for the mechanical configuration was taken from the ARIES-RS design, and detailed CAD renderings were generated. This work (by authors Nelson and Fogarty ) included laying out the envelopes for the flow paths based on a thin flowing first wall stream. (Neil Morley and others at UCLA introduced the idea of a thin flowing first wall with a secondary flow stream for the blanket in APEX by their *Concept for a Li Flowing First wall* or CLIFF.)

Our approach has been to identify design issues as we proceed and specify as much detail as possible while proceeding to develop and improve our conceptual designs. At this point the mechanical features of the divertor include the flow paths and the ducts for pumping and exhaust (see Fig. 1). We expect that the exhaust duct at the bottom will include an electromagnetic pump to assist in evacuating the liquid metal from the chamber. Preliminary work on this has only begun recently and is not reported here.

From our preliminary considerations of plasma edge interactions and basic power handling, Sn as a coolant for a single stream first wall and divertor shows promise. This is an important conclusion as far as it goes; however, we recognize that the all important issue of MHD effects on flow has not yet been treated effectively.

In this iteration of our divertor design, the flow deflector was moved so that it redirects the outboard flow downward before the flow intercepts the divertor heat flux. (In the earlier design in Fig. 1, the deflector is low in the divertor.) This location at the bottom of the first wall provides two advantages. First, it modifies the surface layer of the first wall stream. Since the deflector will also need to redirect flow around a pump duct, we hope that the design can both provided this

redirection and thermal mixing of the heated top layer. Second, the deflection of the stream above the divertor means that a more steeply inclined target angle in the divertor with a lower peak heat load is possible.

Fig. 9 shows four examples of the possible position of a deflector. In each case, the top of the divertor flow was set and then a factor (defined below) that represented how rapidly the surface temperature would increase along the flow length was evaluated as a function of the angle of the diverted flow. (The flux surfaces in the private flux region are omitted here.) The "incline" of the divertor flow is defined here as the downward angle between the flow surface and the horizontal. The "reference point" for case 1 is at  $Z=-2.7\text{m}$ . Here the flow parallel to SOL10 is at an incline of  $43.9^\circ$ . For each case studied, the divertor incline was varied from  $43.9^\circ$  to a maximum angle where the divertor flow reached the separatrix at a  $Z$  of  $-4.5$ . These maximum angles are depicted in Fig. 9.

The criterion of interest here is a relative measure of how fast the temperature of the surface will rise. Our is based on simple 1-D heat transfer equation for heating of a flat surface. The duration of the heating, i.e., the transit time,  $t$ , of fluid in the heated region of the divertor, is inversely proportional to the flow velocity,  $v$ , and to the sine of the angle between the divertor surface and the flux surface. The intensity of the heat load is inversely proportional to the amount of flux expansion (fexp) and to the sine of the angle, and  $q^*$  is the heat load that would be intercepted by a surface perpendicular to the poloidal plane in Fig. 9.

For a solid surface, the spreading of the heat over the inclined area would simply be  $q$  equal to  $q^*$  times  $\sin(\theta)/\text{fexp}$ . However, the relationship for a flowing liquid is somewhat different.

$$T_{\text{rise,surf}} \cong \frac{q}{k} \sqrt{\frac{kt}{\Pi}} \cong q^* \sin(\theta) \sqrt{\frac{1}{\Pi k \rho C_p v}} \sqrt{\frac{L_0}{\sin(\theta)}} \quad \text{with} \quad t = \frac{L_0 \text{fexp}}{\sin(\theta)v}$$

$$T_{\text{rise,surf}} \propto \sqrt{\sin(\theta) \text{fexp}}$$

The expression proportional to the square root of the product of the sin and the flux expansion is the "T-factor" that is plotted in Fig. 10. The flux expansion factor here is evaluated where the divertor flow intercepts the separatrix since this will be the location of the highest heat load. The lowest T-factor in each case occurs when the angle is the smallest, with the separatrix intercept a  $Z=-4.5\text{m}$ , so the flux expansion is the same for the bottom point on each curve and the difference is equal to the square root of the sin of the angle.

Although deflector position 4 achieves the lowest T-factor, the deflector plate must be well into the SOL and some diverted plasma hits upstream of the deflector. While this might be acceptable, we think a more prudent approach is to place the deflector back in the SOL to mitigate possible damage. Also, with regard to MHD effects, we are trying to place the deflector at a position that fluid envelope in the first wall stream can follow a flux surface until the stream is intercepted by the deflector. A better location is position 5 (Fig. 9) with the first

wall flow further out from the plasma. This achieves the same downward trajectory as with deflector position 2 ( $Z=-2.9$ ,  $R=4.8382$ ), but the deflector will further away from the plasma.

Obviously this is not a complete picture of a divertor configuration. What we are reporting here are elements of our work to date that will contribute to the development of a more complete picture.

### **Closing Remarks and Acknowledgements**

A goal of the APEX and ALPS Programs in the US is to investigate the potential for the use of free liquid surfaces in fusion chamber technology. And to do so with a great enough level of effort so that the design issues can be resolved and an accurate assessment of this potential can be understood.

In the ARIES/CLIFF design, we are trying to develop a specific detailed design in which we can identify and solve practical problems associated with the use of liquid surfaces. In this work we are supported by the APEX and ALPS Teams and there is a significant programmatic commitment that enables us to utilize diverse expertise in plasma edge modeling, advanced mechanical and systems design, and heat transfer. We are now still at the beginning stage, but there is progress in identifying useful coolants and divertor geometries and specifying the divertor conditions through plasma edge models.

We again emphasize that the MHD effects on flow must be evaluated to give a realistic rendering of the flow streams in the chamber. We are evaluating other aspects of the divertor configuration while in parallel there is ongoing development by others on the APEX Team of the modeling tools needed for the evaluation of these complicated liquid metal MHD-controlled flows. Readers interested in that ongoing development may wish to check the APEX website[1] for information and references.

### **References**

1. M. Abdou et al., "Exploring novel high power density concepts for attractive fusion systems," *Fus. Eng. & Des.* 45 (1999) 145; many APEX presentations are available on <<http://www.fusion.ucla.edu/APEX/>>
2. R. Mattas and ALPS Team, "ALPS - Advanced Limiter-Divertor Plasma Facing Systems," *Fus. Eng. & Des.* 49-50 (2000) 127
3. M.A. Tillack et al., "Engineering Design of the ARIES-RS Power Plant," *Fusion Eng. & Des.* 41 (1998) 491; also <<http://aries.ucsd.edu/PUBLIC/ariesrs.html>>
4. R.E. Nygren et al., "CLIFF/ARIES - A Liquid Surface Fusion Chamber Design," at 6th Int. Symp. on Fusion Nucl. Tech., San Diego, CA, USA 2002
5. J.C.R. Hunt, Hancox, "The use of liquid lithium as a coolant in a toroidal fusion reactor, Part 1: calculation of the pumping power," CLRM-115, Culham Laboratory (1971)

6. M.A. Hoffman, "Magnetic Field Effects on the Heat Transfer of Potential Fusion Reactor Coolants," UCRL-73993 (1972)
7. B. Badger, *UWMAK-I, A Wisconsin Toroidal Fusion Reactor Design*, University of Wisconsin, UWFD-68, 1973
8. L. Golubchikov, "Development of a Liquid-Metal Fusion-Reactor Divertor with a Capillary-Pore System," JNM, 237 (1976) 667-672
9. J.H. Pitts, "A Consistent HYLIFE Wall Design that Withstands Transient Loading Conditions," 4th ANS Topical Mtg. On the Technology of Controlled Nuclear Fusion, King of Prussia, PA, Oct. 14-17, 1980
10. E. Muraviev, "Contact Devices for Divertor and Limiter Systems of Tokamak Reactors. I. Devices with LM Working Surface," *Voprosy Atomnoi Nauki I Tekhniki, Ser. Termoyaderniy Sintez*, 2, (1980) 57-64
11. W. Wells, "A System For Handling Divertor Ion and Energy Flux Based on a Lithium Droplet Cloud," *Nuclear Technology/Fusion*, 1, (1981) 120
12. V. Baranov, "Liquid Metal Film Flow for Fusion Application," 7th Beer Sheva International Seminar on Liquid Metal Magnetohydrodynamics, 1983
13. A. Bond, "A Liquid Metal Protected Divertor for a Demo Reactor," 13th Symposium on Fusion Technology, Varese, Italy, (1984) 1225
14. B. Karasev, "LM Contact Divertor for INTOR Tokamak Reactor," 4th All-Union Conf. on Engineering Problems of Fusion Reactors, Leningrad, (1988) 225-256
15. V. Vodyanyuk, "Liquid Metal Tokamak Limiter - Problem Definition and First Results," *Plasma Physics*, 14, (1988) 628
16. I. Kirillov, "Alternate Concepts of the Divertor Targets Working Materials to the ITER," October 1990, ITER-IL-PC-8-0-18
17. C. Liao, "A Feasibility Assessment of Liquid-Metal Divertors," *Fusion Technology*, 21, (1992) 1845-1851
18. S. Mirnov, "Liquid-Metal Tokamak Divertors," JNM, 196, (1992) 45-49
19. V. Chuyanov, "Advanced Divertor Plates System Development Proposal," ITER EDA Memo, 1994
20. E. Muraviev, "Liquid-Metal-Cooled Divertor for ARIES," *Fusion Engineering and Design*, 29 (1995) 98-104
21. E. Muraviev, "Open Surface MHD Flow of Liquid Metal Coolant in a Rotating Divertor Target of a Tokamak Fusion Reactor," *Magnetohydrodynamics*, 31 (1995) 306
22. V. Pistunovich, "Research of the Capillary Structure Heat Removal Efficiency Under Divertor Conditions," JNM, 237, (1996) 650-654
23. M.A. Mahdavi, M. Schaffer, "Heat Removal with a Liquid Pellet Curtain" (paper), *Innovative Confinement Concepts Workshop* held at Princeton Plasma Physics Laboratory, April 1998.
24. Ga in T-10 (need reference)
25. T.D. Rognlien, M.E. Rensink, "Interactions between liquid-wall vapor and edge plasmas," JNM 290-293 (2001) 312-316

26. T.D. Rognlien and M.E. Rensink, "Edge-plasma properties in liquid-wall environments," 8th Int. Workshop on Edge Plasma Theory in Fusion Devices, Helsinki, Finland, Sept. 10-12, 2001
27. J.N. Brooks, D. Naujoks, Physics of Plasmas 7 (2000) 2565
28. D. Naujoks, J.N. Brooks, JNM. 290-293(2001)1123.
29. S.S. Smolentsev, M. Abdou, N. Morley, A. Ying, T. Kunugi, "Application of the K-epsilon Model to Open Channel Flows in a Magnetic Field," Int. J. of Eng. Sci., accepted for publication (2001).
30. S.Smolentsev, M. Abdou, T. Kunugi, "Development and Adjustment of K-epsilon Turbulence Model for MHD Channel Flows with Large Aspect Ratio in a Transverse Magnetic Field," Proc. 4<sup>th</sup> Int. PAMIR Conf. on Magneto-hydrodynamics at Dawn of Third Millennium, Giens, France, 1 (2000) 21-26
31. R. Hultgren, R.L. Orr, P.D. Anderson and K.K. Kelly, Selected Values of Thermodynamic Properties of Metals and Alloys, John Wiley & Sons (1963)
32. Y.S. Touloukian, Thermophysical Properties of Matter, Vol. 4, Specific Heat of Metallic Elements and Alloys, IFI-Plenum (1970)
33. T. Iida and R.I.E. Guthrie, The Physical Properties Liquid of Metals, Clarendon, Oxford, 1988.
34. O. Kubaschewski and C.B. Alcock, "Metallurgical Thermochemistry," Pergamon, Oxford, Table C1, p336
35. C.Y. Ho, R.W. Powell, P.E. Liley, J. Physical and Chemical Reference Data, 3 (1974)
36. Cusack and Enderby, Proc. Phys. Soc., 75 p395, cited in Iida[3], Table 8.1 p232

## Figures

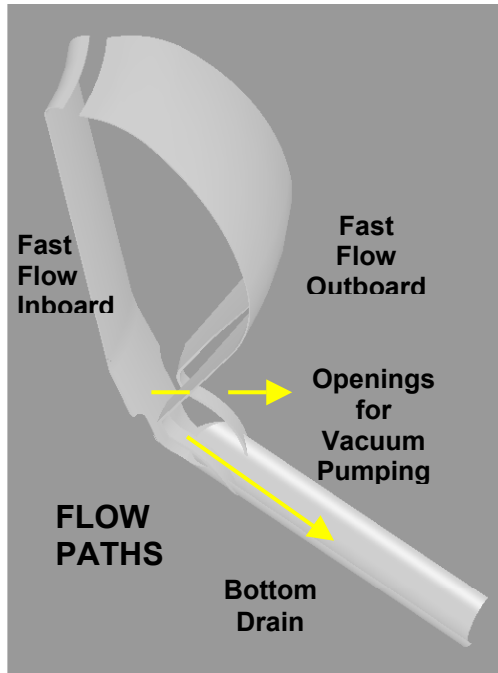


Fig 1. ARIES/CLIFF FW and divertor flow paths

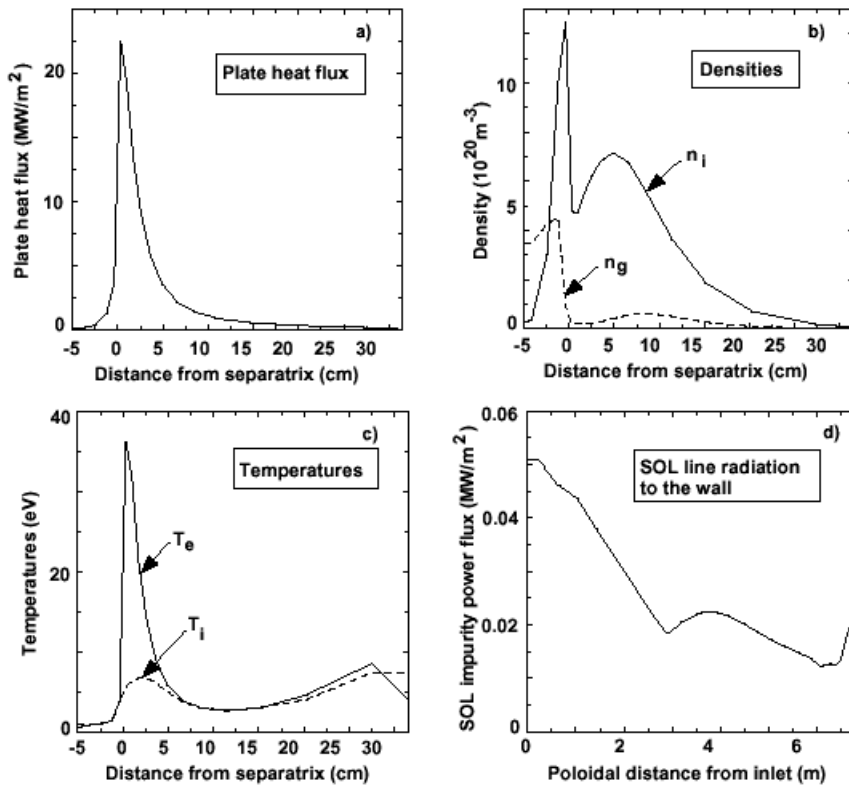


Fig. 2 Temperature windows for LM operation in ARIES/CLIFF

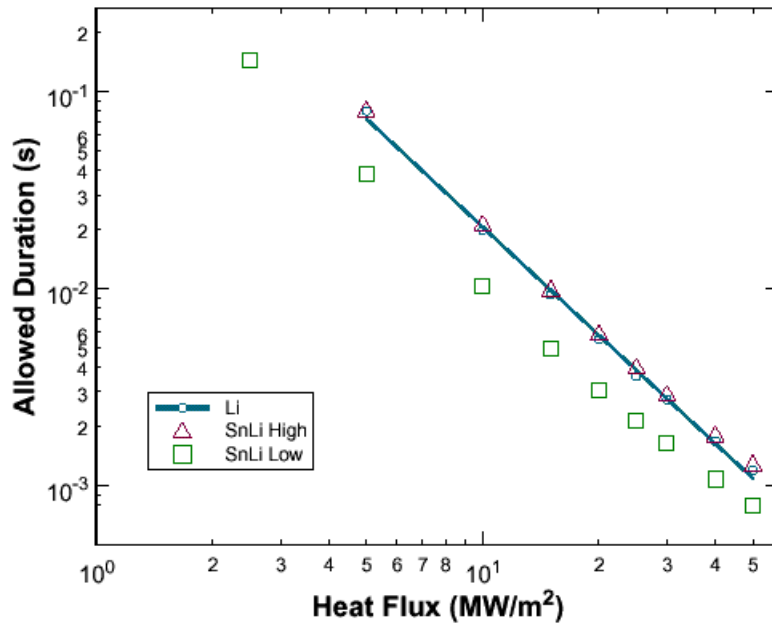


Fig. 3. The allowed duration of heat flux on a flowing liquid surface is shown as a function of the heat flux. High and low estimates for Sn-Li are shown (see text). The slope of the curve is  $-2$ .

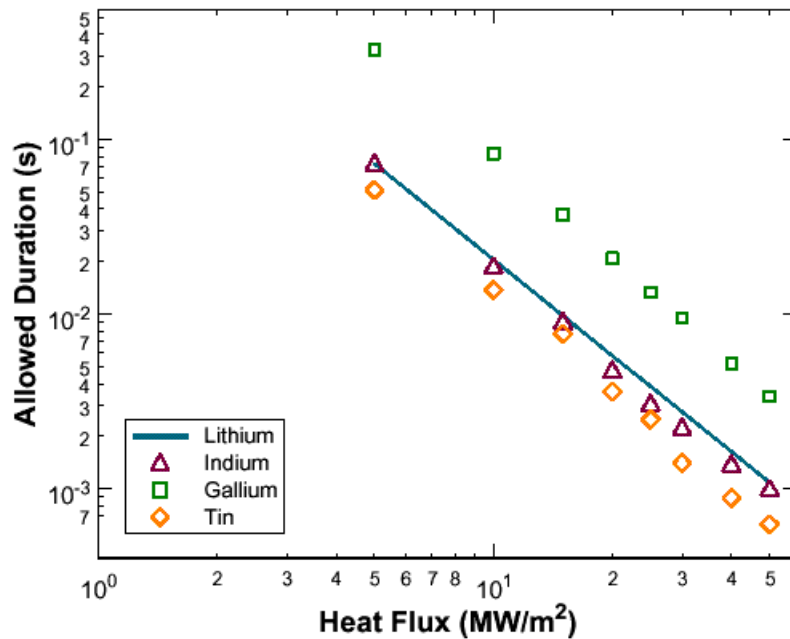


Figure 4. Calculated allowed duration of heat flux for the case of the lower bound temperature limits for Ga, In and Sn compared to the values for Li.

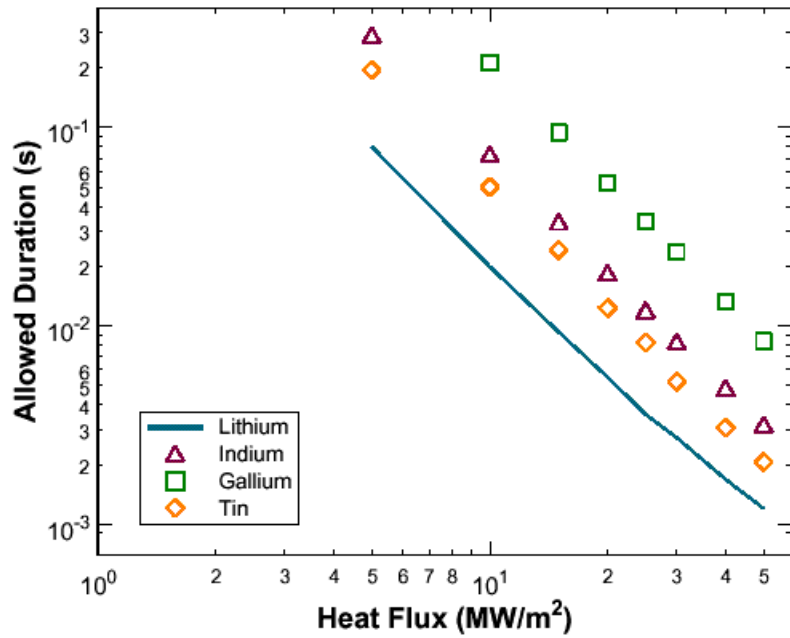


Figure 5. Calculated allowed heat flux duration for the upper bound temperature limits (see text) for Ga, In and Sn compared to the value for Li.

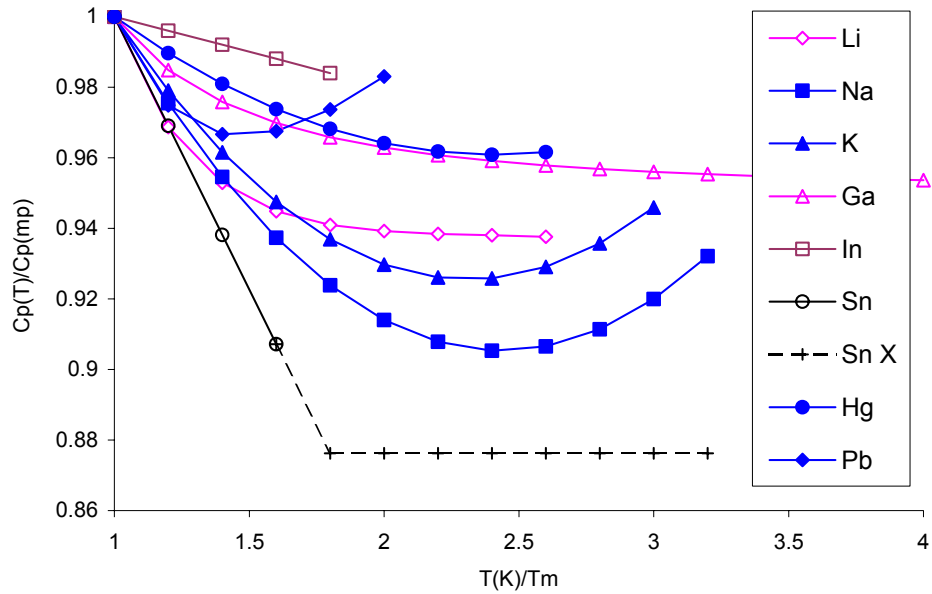


Fig. 6. Trend curves showing the value of  $C_p$  at the temperature indicated divided by  $C_p$  at the melting temperature versus temperature.

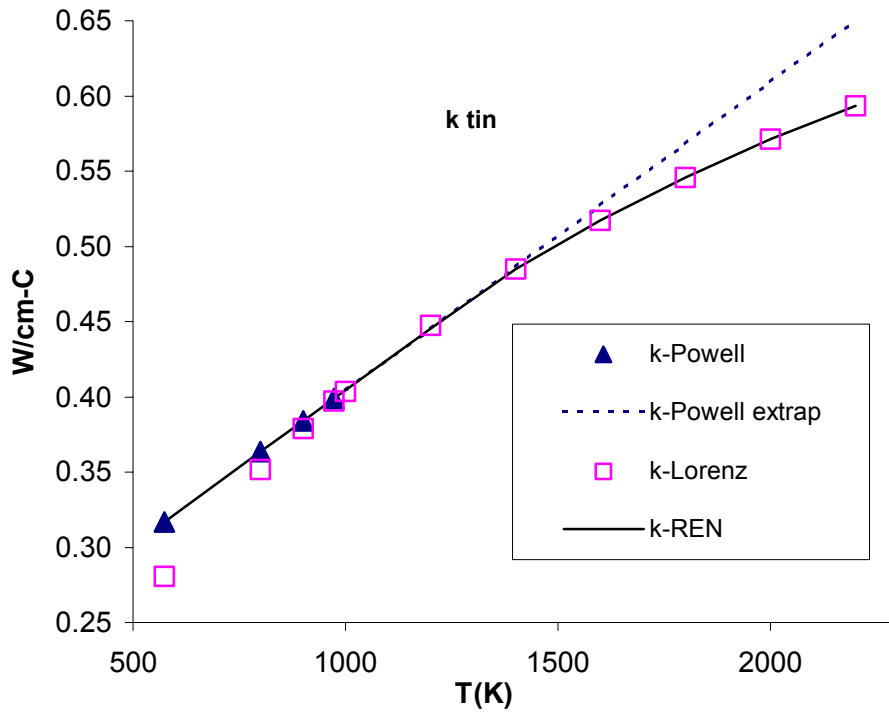


Figure 7. Values of thermal conductivity of liquid Sn versus temperature. The solid line indicates the expression preferred by Nygren.

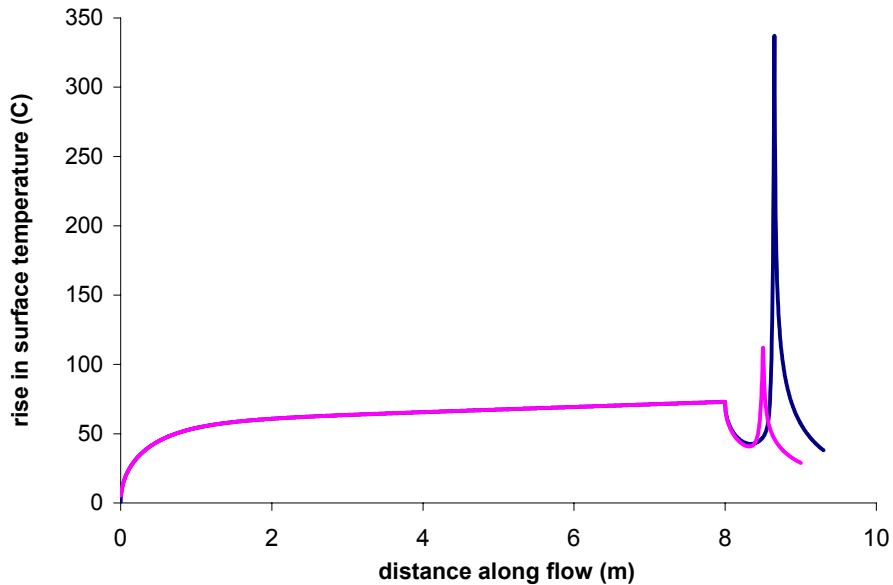


Figure 8. Rise in surface temperature versus distance along the flow stream for a Flibe first wall that receives  $2\text{MW/m}^2$  and an outer divertor that receives  $55\text{MW/m}^2$ . The inner divertor profile is also superimposed. See text regarding temperature decrease at bottom of first wall.

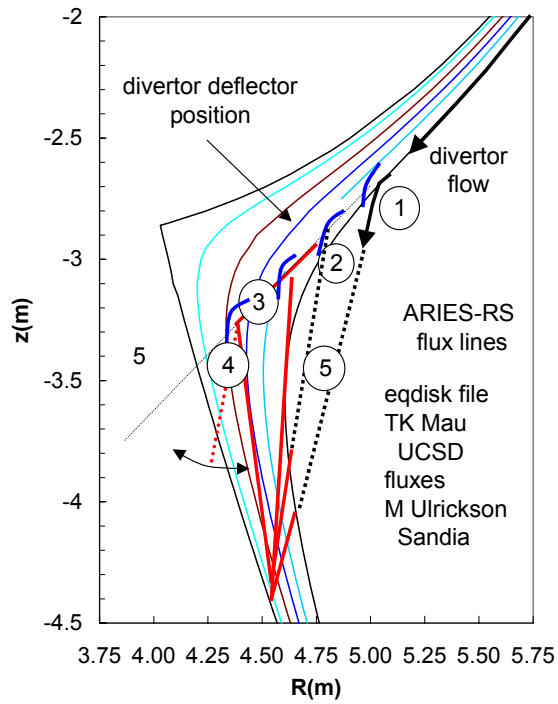


Fig. 9. Flux lines for ARIES-RS and positions of a divertor target used for analysis.

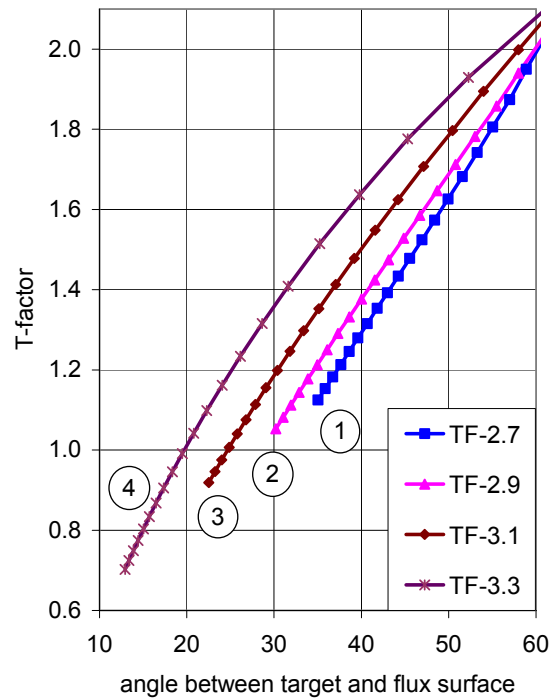


Fig. 10. T-factors for various divertor cases.